

# RECENT ACHIEVEMENTS IN THE PRODUCTION OF METALLIC ION BEAMS WITH THE CAPRICE ECRIS AT GSI

A. Andreev\*, M. Galonska, R. Hollinger, R. Lang, J. Mäder, F. Maimone  
GSI Helmholtzzentrum für Schwerionenforschung, Darmstadt, Germany

## Abstract

The GSI CAPRICE Electron Cyclotron Resonance Ion Source (ECRIS) provides highly-charged ion beams for various experiments at GSI, enabling the delivery of continuous wave (CW) metallic ion beams with low material consumption, which is crucial for producing high charge state ion beams from rare or extremely rare isotopes such as  $^{48}\text{Ca}$ . These metallic beams are produced utilizing the thermal evaporation technique by resistively heated ovens. Due to the research groups' demand for higher beam intensities and the introduction of new ion species, the CAPRICE ECRIS is now required to deliver increased ion currents of higher charge states, as well as to establish the production of the new beams.

## INTRODUCTION

The CAPRICE Electron Cyclotron Resonance Ion Source (ECRIS) at the High Charge State Injector (HLI) of GSI is routinely used for the production of highly charged ion beams from both gaseous and metallic elements. The latter are produced utilizing the thermal evaporation technique by resistively heated ovens. This technique has been continuously optimized over the years to ensure high beam intensity and stable long-term operation. To ensure stable and reliable metal ion beam production, the ovens undergo a carefully controlled preparation process using a specialized oven preparation stand. Over the past years, significant developments have been made to optimize the production of metallic ion beams with CAPRICE ECRIS at GSI, improving both beam intensity and stability. A key focus has been on addressing the challenges associated with the long-term operation of the ECRIS due to material buildup within the plasma chamber, particularly during  $^{48}\text{Ca}$  ion beam operation [1].

A diagnostic tool based on an optical emission spectrometer (OES) installed at the ECRIS at the HLI allows to monitor plasma condition in real time. The diagnostic capabilities of optical emission spectroscopy have been successfully utilized to detect plasma instabilities and to adjust ECRIS parameters accordingly, allowing for improved beam stability and performance. It has been demonstrated that the OES can be used to detect parasitic microwave heating of the oven and identify long-term instabilities during gaseous and metal ion beam operation [1, 2].

Metal ion beams are often requested for various research activities, including those conducted by the Super Heavy Element (SHE) groups. To meet their demand, a test campaign was conducted to establish and improve the production of

high charge states of enriched  $^{54}\text{Cr}$  and  $^{55}\text{Mn}$  ion beams. During the tests, plasma and oven images were captured using a CCD camera to support the operation and enable real-time monitoring of the material consumption. Additionally, the use of a hot screen was investigated to protect the ceramic insulators in the extraction system from metal deposition, thereby improving the operational stability of the ECRIS. This paper describes the operational experience, the intensities and stability achieved for the aforementioned elements.

## EXPERIMENTAL SETUP

### Oven Preparation Stand

To produce metal ion beams, the CAPRICE ECRIS at GSI utilizes resistively heated ovens [3]. This method allows to produce metal ion beam with low material consumption and precise control over the evaporation rate, contributing to the stability and reproducibility of the beam. Before beam operation, the ovens are conditioned in a dedicated oven preparation stand, which allows to perform a controlled heating of the ovens in a vacuum environment. This conditioning process allows to remove residual gases and contaminants from the ovens, ensuring optimal conditions for material evaporation. It allows to improve the stability of the ion beam and extends the operational lifetime of the ovens and minimize downtime during the accelerator operation.

The oven preparation stand has recently undergone a redesign to further improve its functionality and efficiency. Figure 1 shows a photograph of the redesigned stand. It is



Figure 1: Photograph of the oven preparation stand.

equipped with airlocks that enable conditioning of several ovens simultaneously, increasing the operational efficiency. To further improve control over the oven preparation process, it is planned to equip the stand with a camera monitoring

\* a.andreev@gsi.de

system, which will provide a real-time visual feedback during conditioning. Additionally, a residual gas analyzer will be integrated for precise analysis and control of the gas and vapor composition.

### Optical Emission Spectroscopy

To monitor the plasma condition in real time, the OES is used in conjunction with the plasma and oven images provided by a CCD camera [4]. Using the NIST database [5] the emission lines corresponding to the element of interest can be identified. Observing time variations of their intensity provides information about the internal plasma condition during the ECRIS operation and allows for real-time adjustments to the ECRIS operating parameters, ensuring high-intensity and stable beam production. The use of this diagnostic setup was investigated during the tests with  $^{54}\text{Cr}$  and  $^{55}\text{Mn}$ , aiming to support the ECRIS operation.

Due to the relatively high vapor pressure of Cr, the operational temperatures of the oven were required to be around 1500 degrees Celsius, utilizing more than 40 W of heating power. Within this temperature range, the emission spectrum in the visible wavelength domain is mainly characterized by thermal radiation from the oven. As a result, it was not possible to clearly identify individual emission lines of Cr in the measured wavelength range.

During  $^{55}\text{Mn}$  beam operation, the emission line at 810 nm was monitored to estimate the amount of material present in the plasma. Additionally, the infrared part of the spectrum, specifically around 827 nm, was tracked to estimate the relative oven temperature (see Fig. 2). This allows to detect parasitic heating of the oven caused by coupled microwaves, which can affect the material production rate and degrade the ion beam stability. Combined with the oven conditioning process, this approach, as previously reported for  $^{48}\text{Ca}$  ion beam operation [1], has proven effective for optimizing ECRIS performance and ensuring long-term operational stability.

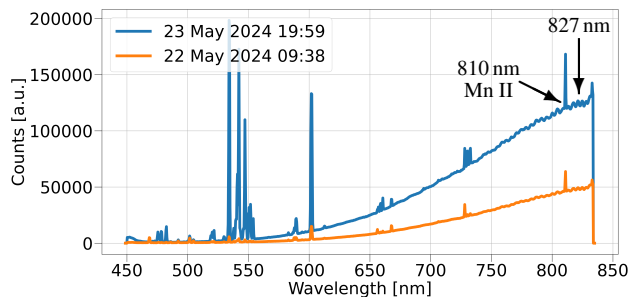


Figure 2: Example for OES measurements during  $^{55}\text{Mn}$  ion beam operation.

## EXPERIMENTAL RESULTS

### Chromium Ion Beam

The recent measurement campaign focused on establishing and improving the production of high charge states of enriched  $^{54}\text{Cr}$  ion beam. While the CAPRICE ECRIS at

GSI has been successfully used to produce  $^{54}\text{Cr}$  ion beams at lower charge states, such as  $^{54}\text{Cr}^{7+}$  and  $^{54}\text{Cr}^{8+}$  [3], this campaign aimed to meet the demand for higher charge states.

Based on prior short-term tests and previous Cr beam times, the desired target intensity  $50\ \mu\text{A}$  of  $^{54}\text{Cr}^{10+}$  was set. Figure 3 shows the intensity of  $^{54}\text{Cr}^{10+}$  measured during three days of the ECRIS operation with helium as a support gas. The desired target intensity was reached at the beginning

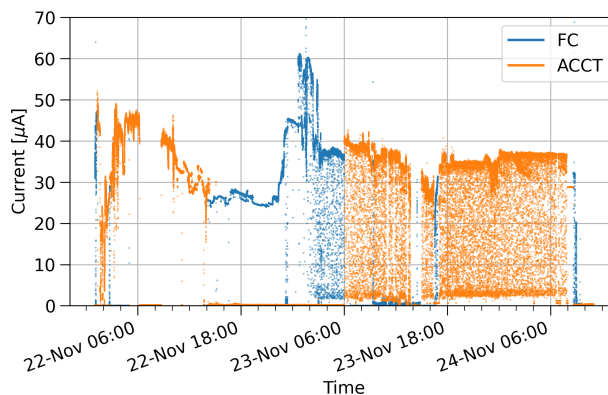


Figure 3:  $^{54}\text{Cr}^{10+}$  intensity measured during 3 days of the ECRIS operation. FC denotes measurements taken with a Faraday cup during accelerator maintenance, while ACCT represents measurements from an AC current transformer.

of the ECRIS operation, however the ECRIS performance was impacted by discharges in the extraction system, which appeared on the second day of the ECRIS operation. As their frequency increased over time, the beam stability significantly degraded and the target intensity could not be maintained. A subsequent inspection of the extraction system revealed metal traces deposited on the ceramic insulators in the extraction column (see Fig. 4). An electron microscope

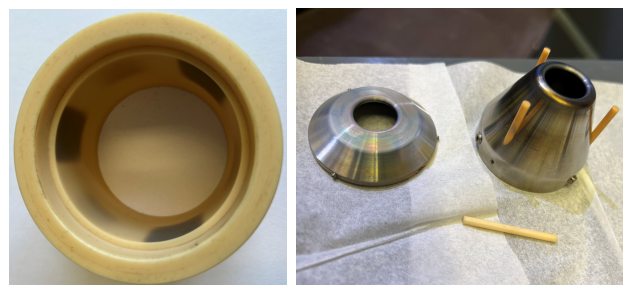


Figure 4: Photographs of ceramic insulators in the extraction column after the  $^{54}\text{Cr}$  operation.

investigation confirmed the presence of chromium, but could not verify if it was the only component. To address this issue and mitigate the metallic buildup on the ceramic surfaces, a series of tests with a hot screen is planned. Similar tests conducted during  $^{55}\text{Mn}$  operation have already demonstrated the effectiveness of the hot screen in improving operational stability, as discussed later in this paper. Figure 5 shows a typical mass-to-charge spectrum of the extracted ion beam. The overall consumption of  $^{54}\text{Cr}$  material was 8 mg/h on average (without material recycling).

Content from this work may be used under the terms of the CC BY 4.0 license (© 2024). Any distribution of this work must maintain attribution to the author(s), title of the work, publisher, and DOI

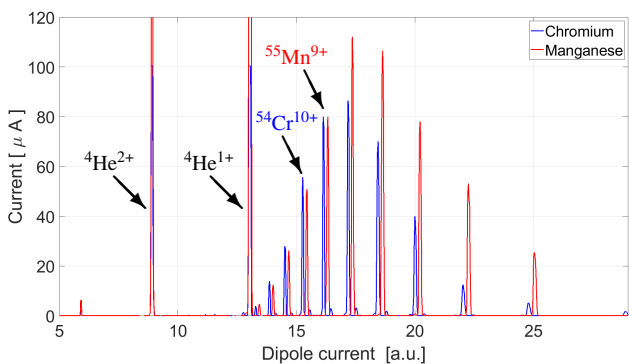


Figure 5: Mass-to-charge spectra of  $^{54}\text{Cr}$  (blue) and  $^{55}\text{Mn}$  (red), optimized for  $^{54}\text{Cr}^{10+}$  and  $^{55}\text{Mn}^{9+}$ , respectively.

The possibility of using a tungsten mesh to prevent parasitic microwave heating of the oven, a technique that was previously successful for  $^{48}\text{Ca}$  operation [4], was tested. Although the ECRIS operation was more stable with the mesh installed, the build-up of condensed material on the mesh led to reduced  $^{54}\text{Cr}^{10+}$  intensity indicating that this approach may not be optimal for long-term Cr operation. Figure 6a shows a photograph of the tungsten mesh after  $^{54}\text{Cr}$  beam operation.

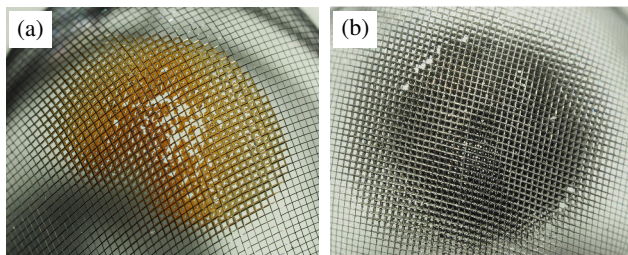


Figure 6: Photographs of the tungsten meshes after  $^{54}\text{Cr}$  (a) and  $^{55}\text{Mn}$  (b) operation.

### Manganese Ion Beam

The beam establishment tests were conducted at the EIS test bench to produce the  $^{55}\text{Mn}$  ion beam for the first time using the CAPRICE ECRIS at GSI. The aim of this test campaign was to determine the achievable beam intensity of higher charge states for  $^{55}\text{Mn}$ , with a focus on  $^{55}\text{Mn}^{9+}$  production.

The intensity of  $^{55}\text{Mn}^{9+}$  beam measured during the three day beam establishment test with the hot screen installed and helium as a support gas is shown in Fig. 7. An average intensity of  $80\ \mu\text{A}$  was achieved for  $^{55}\text{Mn}^{9+}$ . Similar to the  $^{54}\text{Cr}$  beam tests, discharges appeared in the extraction system on the second day of ECRIS operation. However, their frequency was low enough to maintain stable operation and production of  $^{55}\text{Mn}^{9+}$  beam. The use of the hot screen improved beam stability and delayed the onset of discharges, enabling stable operation at high intensities with minimal disruptions. A typical mass-to-charge spectrum for  $^{55}\text{Mn}$  obtained during the tests is shown in Fig. 5. The overall average consumption of  $^{55}\text{Mn}$  material was  $8.1\ \text{mg/h}$  (without material recycling).

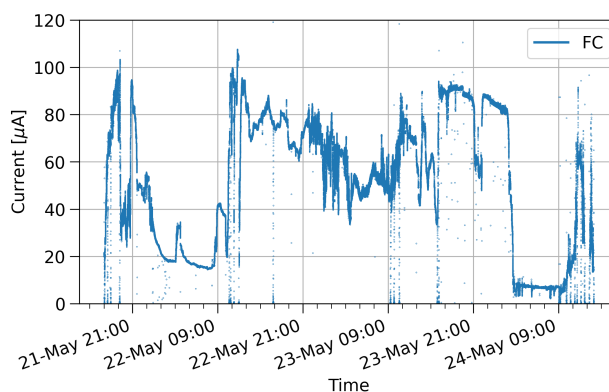


Figure 7:  $^{55}\text{Mn}^{9+}$  intensity measured during 3 days of the ECRIS operation.

In addition to the hot screen tests, experiments with a tungsten mesh were also carried out. During  $^{55}\text{Mn}$  operation the mesh was completely clogged with a condensed material after one day of the ECRIS operation, preventing further  $^{55}\text{Mn}$  evaporation and beam production (see Fig. 6b).

### OES Results with Manganese Ion Beam

During the  $^{55}\text{Mn}^{9+}$  ion beam establishment tests, the OES was employed to monitor plasma condition and detect parasitic heating effects of the oven. The time variations of two specific emission lines were monitored: the Mn II emission line at  $810\ \text{nm}$  and an emission line at  $827\ \text{nm}$ , closer to the infrared part of the optical spectrum, which was selected to estimate the relative oven temperature (see Fig. 2).

Figure 8 presents the time variations of key ECRIS parameters and normalized emission line intensities. Both figures, show the  $^{55}\text{Mn}^{9+}$  ion beam current, along with oven current and reflected microwave power in Fig. 8a, and ion source pressure and drain current of the extraction power supply in Fig. 8b.

In both cases, the OES data reveal a strong correlation between the intensity of the Mn II emission line and the  $^{55}\text{Mn}^{9+}$  beam current. The emission line at  $827\ \text{nm}$  shows clear variations in response to changes in the oven temperature, indicating parasitic heating of the oven due to coupled microwave power. As the reflected power decreases (see Fig. 8a), the oven temperature increases, leading to a higher production rate of  $^{55}\text{Mn}$ , as reflected by the rising intensity of the Mn II emission line and a corresponding increase in the  $^{55}\text{Mn}^{9+}$  ion beam current. These changes in reflected power also correlate with periodic minima and maxima in the oven current. A decrease in reflected power indicates a stronger microwave coupling, with a portion of the microwave power heating the oven. As the oven temperature rises, its resistance increases, leading to a reduction in the current flowing through the oven. When reflected power increases again, the oven cools down, resulting in a decrease in both the Mn II emission line intensity and the ion beam current.

In Fig. 8b, a similar relationship between the  $^{55}\text{Mn}^{9+}$  beam current and the emission line intensities can be observed,

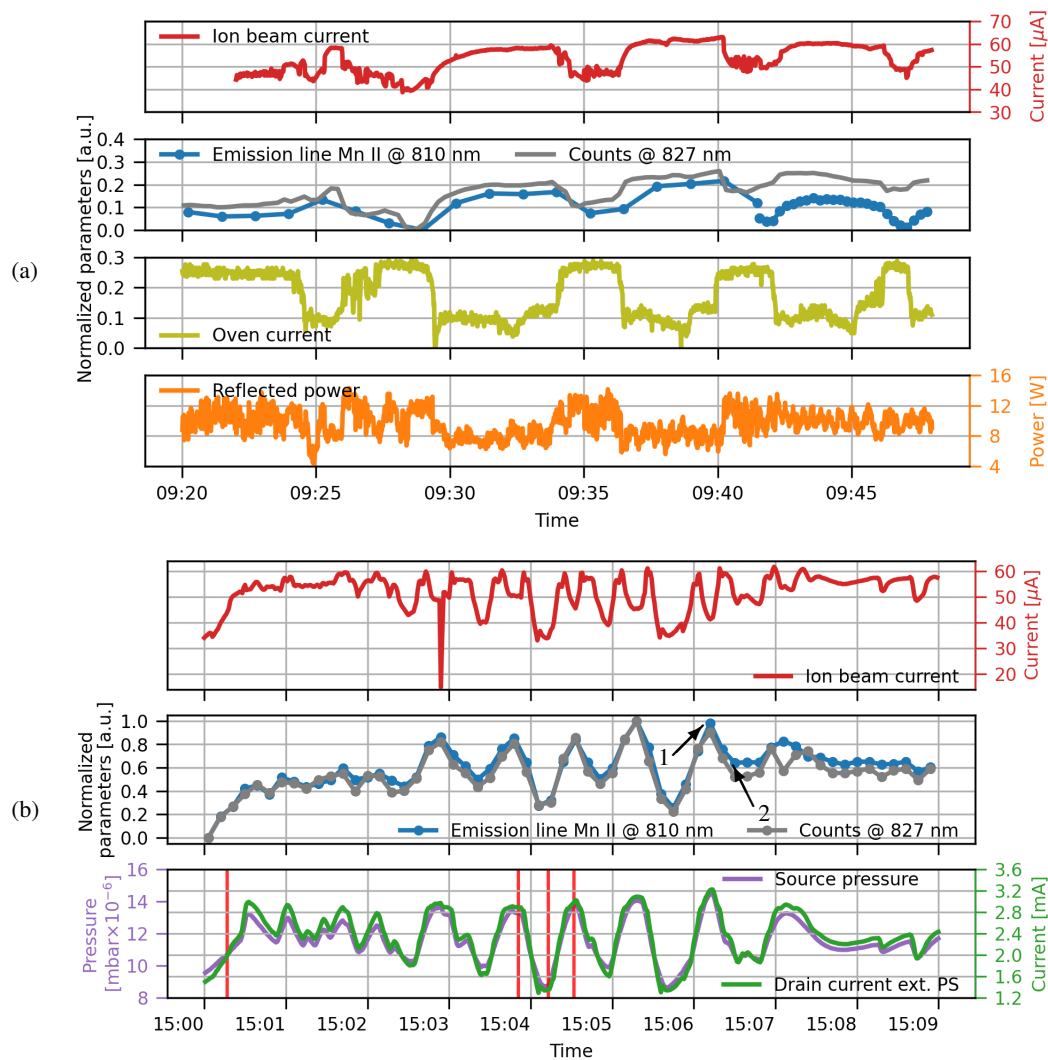


Figure 8: Time variations of selected emission lines and ECRIS parameters illustrating (a) the effect of parasitic heating of the oven by coupled microwaves, (b) ion source pressure variations. The red vertical lines mark the time when the gas valve settings were changed. The time instants marked as (1) and (2) correspond to the CCD images shown in Fig. 9.

together with the influence of the source pressure. The beam current shows a local minimum at the maxima of the Mn II emission line, which can be explained by a shift of the plasma's charge state distribution towards lower charge states. The red vertical lines in the figure indicate the moments when the gas valve settings were manually adjusted, leading to corresponding changes in the source pressure.

Additionally, plasma images taken at the local maxima and minima of the emission lines visually confirm the beam intensity variations (see Fig. 9). The brighter plasma image corresponds to a higher total extracted ion beam current, while the darker image indicates reduced beam intensity.

These results highlight the role of OES and CCD plasma and oven imaging as a real-time diagnostic tools for monitoring plasma conditions and detecting parasitic oven heating effects. They provide a feedback on plasma condition enabling better control of the ECRIS operating parameters and allowing to improve the beam intensity and stability.

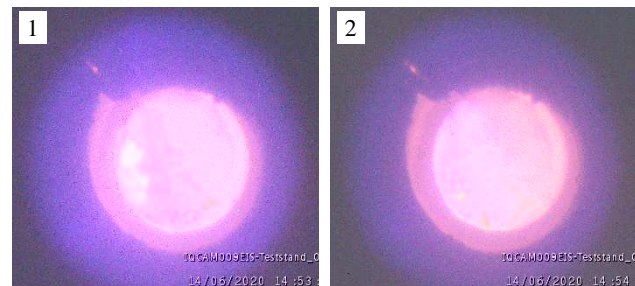


Figure 9: CCD images of the plasma during <sup>55</sup>Mn ion beam operation. Annotations (1) and (2) correspond to the time instants marked in Fig. 8b.

## ACKNOWLEDGEMENTS

The authors would like to thank Michael Wagner from the GSI Materials Research Department for his support in performing the SEM EDX investigation.

## REFERENCES

- [1] F. Maimone *et al.*, “Stable and intense  $^{48}\text{Ca}$  ion beam production with a microwave shielded oven and an optical spectrometer as diagnostic tool”, in *Proc. ECRIS'20*, East Lansing, MI, USA, Sep. 2020, pp. 50-53.  
doi:10.18429/JCoW-ECRIS2020-MOZZ003
- [2] F. Maimone *et al.*, “Research and development activities to increase the performance of the CAPRICE ECRIS at GSI”, *J. Phys.: Conf. Ser.*, vol. 2743, p. 012048, 2024.  
doi:10.1088/1742-6596/2743/1/012048
- [3] K. Tinschert, R. Lang, J. Mäder, F. Maimone, and J. Roßbach, “Metal ion beam production with improved evaporation ovens”, in *Proc. ECRIS'12*, Sydney, Australia, Sep. 2012, pp. 140-142.
- [4] F. Maimone *et al.*, “Optical spectroscopy as a diagnostic tool for metal ion beam production with an ECRIS”, *Rev. Sci. Instrum.*, vol. 90, no. 12, p. 123108, Dec. 2019.  
doi:10.1063/1.5127571
- [5] NIST Atomic Spectra Database Lines Form,  
[https://physics.nist.gov/PhysRefData/ASD/lines\\_form.html](https://physics.nist.gov/PhysRefData/ASD/lines_form.html)